Received: 26 November 2016 | Revised: 27 January 2017 | Accepted: 2 February 2017

DOI: 10.1002/aoc.3781

FULL PAPER

WILEY Applied Organometallic Chemistry

Green synthesis of reduced graphene oxide/Fe_3O_4/Ag ternary nanohybrid and its application as magnetically recoverable catalyst in the reduction of 4-nitrophenol

Tran Viet Thu[1,2]† | **Pil Ju Ko**[3]† | **To Van Nguyen**[2] | **Nguyen Thanh Vinh**[2] | **Doan Minh Khai**[2] | **Le Trong Lu**[4]

[1] Institute of Research and Development, Duy Tan University, K7/25 Quang Trung, Danang 550000, Vietnam

[2] Department of Chemical Engineering, Le Quy Don Technical University, 236 Hoang Quoc Viet, Hanoi 100000, Vietnam

[3] Department of Electrical Engineering, Chosun University, 375, Seosuk-dong, Dong-gu, Gwangju 501-759, Republic of Korea

[4] Institute for Tropical Technology, Vietnam Academy of Science and Technology, 18 Hoang Quoc Viet, Cau Giay, Hanoi, Vietnam

Correspondence
Tran Viet Thu, Institute of Research and Development, Duy Tan University, K7/25 Quang Trung, Danang 550000, Vietnam.
Email: thutv.ltu@gmail.com

Funding Information
Vietnam National Foundation for Science and Technology Development (NAFOSTED), Grant/Award Number: 103.02-2015.100; Le Quy Don University, Grant/Award Number: 14.0.A.04

Materials having both magnetic and catalytic properties have shown great potential for practical applications. Here, a reduced graphene oxide/iron oxide/silver nanohybrid (rGO/Fe_3O_4/Ag NH) ternary material was prepared by green synthesis of Ag on pre-synthesized rGO/Fe_3O_4. The as-prepared rGO/Fe_3O_4/Ag NH was characterized using Fourier transform infrared spectroscopy, X-ray diffractometry, Raman spectroscopy, vibrating sample magnetometry, transmission electron microscopy and energy-dispersive X-ray spectroscopy. rGO sheets were covered with Fe_3O_4 (8–16 nm) and Ag (18–40 nm) nanoparticles at high densities. The mass percentages were 13.47% (rGO), 62.52% (Fe_3O_4) and 24.01% (Ag). rGO/Fe_3O_4/Ag NH exhibited superparamagnetic behavior with high saturated magnetization (29 emu g^{-1} at 12 kOe), and efficiently catalyzed the reduction of 4-nitrophenol (4-NP) with a rate constant of 0.37 min^{-1}, comparable to those of Ag-based nanocatalysts. The half-life of 4-NP in the presence of rGO/Fe_3O_4/Ag NH was *ca* 1.86 min. rGO/Fe_3O_4/Ag NH could be magnetically collected and reused, and retained a high conversion efficiency of 94.4% after the fourth cycle. rGO/Fe_3O_4/Ag NH could potentially be used as a magnetically recoverable catalyst in the reduction of 4-NP and environmental remediation.

KEYWORDS
4-nitrophenol, graphene oxide, magnetic nanoparticles, nanocatalyst, silver

1 | INTRODUCTION

Materials that have dual catalytic and magnetic properties have recently attracted much research interest,[1,2] because they provide a promising solution for the easy separation of catalysts from reaction mixtures using an external magnetic field. The separated catalysts can be repeatedly used and recovered for subsequent reaction cycles, making the usage of catalysts more efficient and economic than that of traditional non-recoverable ones. Although the magnetic recovery of catalysts is fascinating, it is important to resolve the activity issue of catalysts because the immobilization of a catalyst on a magnetic material means its active sites are less accessible to reactants. To that end, various magnetic materials have been developed as supports for catalysts.[1,3] Also, to meet the demand of sustainable development and efficient use of resources such as catalysts, it is imperative to develop synthetic routes that produce catalysts having higher activity in greener ways. Therefore, the green synthesis of magnetically recoverable catalysts is a fast-growing field.[1,4]

†These authors contributed equally to this work

Recently, reduced graphene oxide (rGO) has been extensively used as a substrate for various catalysts,[5–9] photocatalysts,[10] electrocatalysts[11] and sensors[12] owing to its unique advantages such as large surface area, high chemical stability, high mechanical strength and flexibility. rGO can be incorporated with a variety of magnetic materials to form magnetic hybrids, of which rGO/Fe_3O_4 is one of the most promising systems due to its ease of synthesis, low cost, strong superparamagnetism, good biocompatibility and low toxicity. rGO/Fe_3O_4 hybrids have been used to deposit various catalytic materials such as Pt,[13] Pd,[14] Au[15,16] and Ag.[17–19] Among these, Au and Ag have attracted tremendous interest due to their interesting properties and potential applications.[20–22] Particularly, the rGO/Fe_3O_4/Ag ternary system has received considerable attention because it exhibits multiple functions, including catalytic activity towards the degradation of rhodamine B[17] and reduction of nitroarenes,[18,19] microwave absorption[23,24] and antibacterial[25] and photothermal antibacterial agent.[26] Considering the increasing importance of this hybrid material, it is necessary to develop novel methods for the synthesis of rGO/Fe_3O_4/Ag which are not only facile and efficient but also environmentally friendly.

To date, several strategies have been developed to address the issue. rGO/Fe_3O_4/Ag hybrids have been prepared by reductive deposition of Ag onto previously synthesized rGO/Fe_3O_4 using $NaBH_4$,[17,23] ammonium formate[25] or NaOH.[18] The incorporation of rGO/Fe_3O_4 with polyethyleneimine was proved to be efficient in facilitating the growth of Ag.[26] Alternatively, rGO/Fe_3O_4/Ag hybrids can be formed by the condensation reaction between NH_2-functionalized Fe_3O_4 nanoparticles (NPs) and ─COOH group on previously synthesized rGO/Ag binary hybrids, using *N*-hydroxysuccinnimide/1-ethyl-3-(3-dimethylamino propyl) carbodiimide as activator.[19] rGO/Fe_3O_4/Ag hybrids can also be synthesized by the solvothermal method using ethylene glycol as solvent and sodium acetate as structure-directing agent at elevated temperature.[24] Though significant progress has been made in the synthesis of rGO/Fe_3O_4/Ag hybrids, it is still needed to develop simpler and greener approaches.

In this paper, we describe a simple, inexpensive and green synthetic route that was developed to produce rGO/Fe_3O_4/Ag nanohybrid (NH). This hybrid is formed by the deposition of Ag NPs onto rGO/Fe_3O_4 hybrid using sodium citrate as reducing agent. Optical, structural, morphological and magnetic properties of the resulting hybrid were comprehensively studied. rGO/Fe_3O_4/Ag NH efficiently catalyzes the reduction of 4-nitrophenol (4-NP) with a rate constant comparable to that of typical Ag-based catalysts. rGO/Fe_3O_4/Ag NH can be magnetically collected and reused multiple times, introducing a convenient and economical way for practical applications.

2 | EXPERIMENTAL

2.1 | Chemicals

Graphite flakes were provided by AMT Co. Ltd. Sulfuric acid (H_2SO_4), sodium hydroxide (NaOH), potassium persulfate ($K_2S_2O_8$), phosphorus pentoxide (P_2O_5), potassium permanganate ($KMnO_4$), hydrogen peroxide (H_2O_2), iron(II) sulfate heptahydrate ($FeSO_4{\cdot}7H_2O$), iron(III) sulfate dihydrate ($Fe_2(SO_4)_3{\cdot}2H_2O$), ammonium hydroxide (NH_4OH), sodium citrate pentahydrate ($Na_3C_6H_5O_7{\cdot}5H_2O$) and ethanol were purchased from Xilong Chemical Co. Ltd. Sodium borohydride ($NaBH_4$) was obtained from Chengdu Jinshan Chemical Reagent Co. Ltd. Silver nitrate ($AgNO_3$) was purchased from Shanghai Experiment Reagent Co. Ltd. All the reagents were of analytical grade and used without further purification.

2.2 | Synthesis of GO/Fe_3O_4

GO/Fe_3O_4 NH was synthesized according to our previously reported procedure.[27] Briefly, we employed a modified Hummer's method to synthesize GO nanosheets.[6] Then, Fe_3O_4 NPs were decorated on the surface of the GO nanosheets through a co-precipitation reaction between Fe^{2+}, Fe^{3+} and OH^- ions (pH = 11). The reaction was carried out at 90 °C for 1 h. The resulting GO/Fe_3O_4 NH was magnetically collected, washed with distilled water and ethanol, and dried at 80 °C in a vacuum oven.

2.3 | Synthesis of rGO/Fe_3O_4/Ag NH

rGO/Fe_3O_4/Ag NH was prepared by reducing Ag^+ ions in boiled sodium citrate solution. In a typical synthesis, 118.3 mg of $AgNO_3$ (0.7 mmol) was dissolved in a dispersion containing 250 mg of GO/Fe_3O_4. An amount of 365.4 mg of $Na_3C_6H_5O_7{\cdot}5H_2O$ (1.05 mmol) was then dissolved in the resulting solution (the $AgNO_3$:$Na_3C_6H_5O_7$ molar ratio was selected as 1.0:1.5). The final solution was brought to the boil and refluxed at that temperature for 1 h. The as-prepared rGO/Fe_3O_4/Ag NH was magnetically separated and subsequently washed with water and ethanol multiple times to remove any excess reactants. Finally, rGO/Fe_3O_4/Ag NH was dried at 80 °C overnight and stored for further characterization and catalytic evaluation. The final rGO:Fe_3O_4:Ag mass ratio was approximately 50 mg:200 mg:75 mg (1.0:4.0:1.5) based on the feed ratio.

2.4 | Characterization

Powder X-ray diffraction (XRD) analysis was conducted with a Siemens D5005 X-ray diffractometer (Cu Kα radiation line, λ = 1.5406 Å; 30 kV/40 mA). The measurements were

performed at a scanning rate of 0.9° min^{-1} (scan step of 0.03°) with 2θ ranging from 10° to 70°. The average crystallite sizes (D_{XRD}) were estimated from the (311) peak (Fe) and (111) peak (Ag) according to the Scherrer formula:

$$D_{XRD} = \frac{K\lambda}{B\cos\theta}$$

where $K = 0.9$ is the Scherrer constant; λ is the wavelength of the incident X-ray beam (1.5406 Å for Cu Kα radiation); θ is the Bragg angle; and B is the full width at half maximum in radians.

Raman spectra were collected with a Horiba Jobin-Yvon LabRam HR800 Raman spectrometer equipped with a 632.8 nm He–Ne laser as the excitation source. UV–visible spectra were recorded with a Varian Cary 50 UV–visible spectrophotometer using 10 mm path length quartz cuvettes. Transmission electron microscopy (TEM) images were obtained using a Jeol JEM-1010 microscope. Samples for TEM were prepared by placing an ethanol suspension of the solid sample on a formvar-coated copper grid followed by drying at room temperature. Scanning electron microscopy (SEM) images and energy-dispersive X-ray (EDX) spectra were collected with a Hitachi S4800 field emission SEM instrument incorporated with a Horiba EMAX EDX analyzer. Fourier transform infrared (FT-IR) spectra were measured in the range 400–4000 cm^{-1} using a PerkinElmer Spectrum Two spectrometer equipped with a universal attenuated total reflectance accessory. The magnetization and hysteresis loops were measured at room temperature using a custom-built vibrating sample magnetometer with an applied magnetic field of −15 to +15 kOe. The vibrating sample magnetometer was calibrated with a ferromagnetic plate made of Ni with known magnetization.

2.5 | Catalytic study

We evaluated the catalytic activity of rGO/Fe_3O_4/Ag NH using the catalytic transformation of 4-NP to 4-aminophenol (4-AP) with $NaBH_4$ as a reducing agent. The catalytic reactions were carried out in a 250 ml beaker. The beaker was first loaded with 10 ml of 4-NP solution (1 mM). Next, 10 ml of catalyst solution (35 mg l^{-1}) was added and stirred. Finally, 80 ml of as-prepared $NaBH_4$ solution (10 mM) was added and vigorously shaken. The final concentrations of 4-NP, $NaBH_4$ and catalyst were 0.1 mM, 8 mM and 3.5 mg l^{-1}, respectively. An amount of 2 ml of final solution was immediately transferred to a 1 cm quartz cell for measurement of time-dependent UV–visible absorption spectra. Upon completion of the measurement, the catalyst was magnetically separated from the reaction solution and washed three times with water for subsequent uses.

3 | RESULTS AND DISCUSSION

3.1 | Formation process of rGO/Fe_3O_4/Ag NH

Figure 1 illustrates the preparation process of rGO/Fe_3O_4/Ag NH. Firstly, GO is prepared by oxidation of graphite in H_2SO_4 and $KMnO_4$ solution using a modified Hummer's

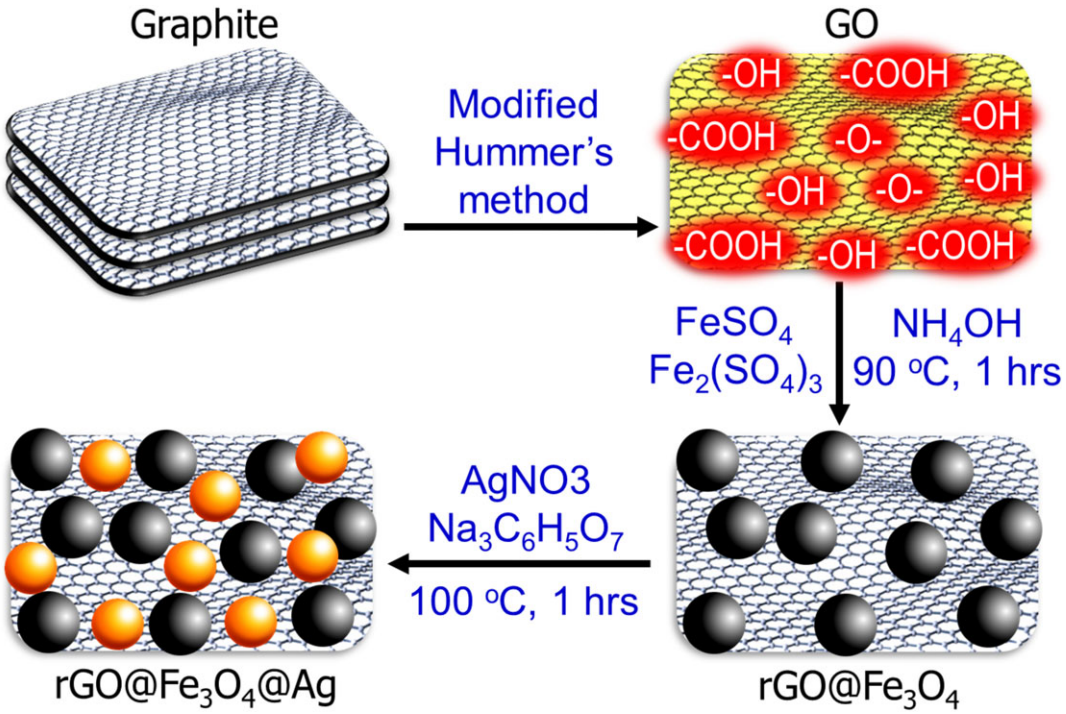

FIGURE 1 Synthesis of rGO/Fe_3O_4/Ag NH

method as described previously.[6,27] GO contains a variety of oxygen-containing functional groups such as —COOH, —COH, ketone, epoxy and —OH, which render GO water-soluble. In the next step, rGO/Fe_3O_4 NH is prepared by the co-precipitation route using GO, $FeSO_4$ and $Fe_2(SO_4)_3$ as precursors. Finally, rGO/Fe_3O_4/Ag NH is formed by deposition of Ag onto the surface of rGO/Fe_3O_4 NH. In this step, Ag(I) ions are adsorbed onto the surface of rGO/Fe_3O_4 by electrostatic bonding, then reduced by citrate ions at boiling temperature. This process also transforms GO to rGO. The several benefits of using sodium citrate include: (a) it is an environmentally friendly reductant; (b) it serves as both reducing agent and capping agent for the simultaneous reduction of GO and silver; and (c) it can prevent the agglomeration of the resulting rGO/Fe_3O_4/Ag NH by disrupting π–π interactions between rGO sheets, similarly to that of rGO/Au NHs.[28]

3.2 | FT-IR spectroscopy

Figure 2 shows FT-IR spectra of GO, GO/Fe_3O_4 and rGO/Fe_3O_4/Ag NH. The presence of various oxygen-containing groups is observed at 3000–3500 cm^{-1} (O—H stretch), 1725 cm^{-1} (carbonyl/carboxyl C═O stretch),[29] 1630 cm^{-1} (vibrations of adsorbed water molecules and unoxidized, aromatic carbon rings), 1400 cm^{-1} (—OH deformation)[30] and 1040 cm^{-1} (alkoxy/epoxy C—O stretch).[31] A very weak and broad absorption band occurring at *ca* 1240 cm^{-1} (C—O—C stretch)[29] indicates that our GO contains negligible amount of ether groups. The absorption bands of O—H stretch are very broad for GO and GO/Fe_3O_4 but become much narrower for rGO/Fe_3O_4/Ag NH (not shown here), indicating that the population of OH-containing groups is significantly decreased during citrate reduction. Stretching vibrations of C═O at 1725 cm^{-1} almost disappear in spectra of GO/Fe_3O_4 and rGO/Fe_3O_4/Ag NH. The peaks at 540 cm^{-1} for GO/Fe_3O_4 and rGO/Fe_3O_4/Ag are attributed to the stretching mode of bonds between tetrahedral and octahedral metal ions and oxide ions.[32] The rest of the peaks are attributed to vibrations of citrate ions. These results clearly indicate the formation of rGO/Fe_3O_4/Ag NH.

3.3 | XRD analysis

Figure 3 shows the typical XRD pattern of rGO/Fe_3O_4/Ag NH. Three prominent peaks at 38.2° (d = 2.36 Å), 44.3° (d = 2.04 Å) and 64.5° (d = 1.44 Å) are well attributed to (111), (200) and (220) lattice planes of crystalline silver (JCPDS no. 04–0783).[6] The characteristic diffraction peaks of rGO are not observed for two reasons: firstly, the crystallinity of rGO is very weak, because restacking of rGO individual sheets is inhibited by Fe_3O_4 and Ag NPs; secondly, the mass ratio of Fe_3O_4 and Ag dominates that of rGO. The broad peaks occurring at 30.1° (d = 2.97 Å), 35.5° (d = 2.52 Å), 43.1° (d = 2.09 Å), 57.2° (d = 1.61 Å) and 62.7° (d = 1.48 Å) are well indexed to (220), (311), (400), (511) and (440) lattice planes of spinel Fe_3O_4 (JCPDS no. 04–0783),[27] indicating the presence of crystalline Fe_3O_4 NPs on rGO substrate. Both Fe_3O_4 and Ag NPs occupy the rGO surface, suppressing the restacking of rGO through steric hindrance. The grain sizes of Fe_3O_4 and Ag NPs, calculated from the peak broadening using Scherrer's formula, are 12.8 and 17 nm, respectively.

3.4 | Raman spectroscopy

Raman spectra of GO and rGO/Fe_3O_4/Ag NH are shown in Figure 4. The Raman spectrum of GO exhibits two prominent bands at 1340 and 1595 cm^{-1}, related to disorder mode due to the oxidation of graphite (D band) and first-order E_{2g} mode from sp^2 carbon domains (G band).[33] An overtone of the D band is also observed at 2680 cm^{-1} (2D band),

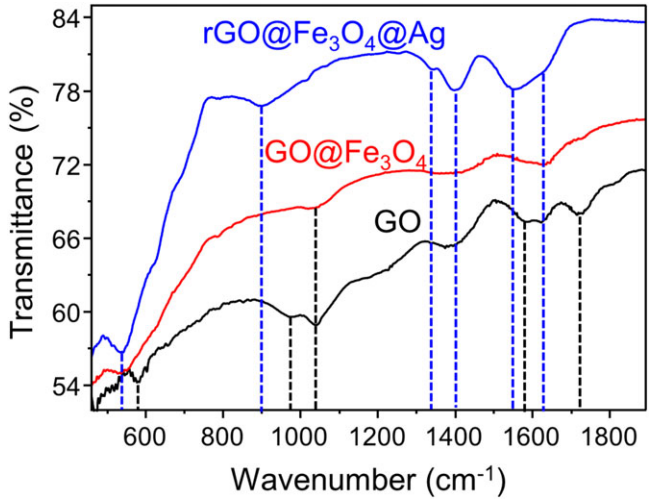

FIGURE 2 FT-IR spectra of GO, GO/Fe_3O_4 and rGO/Fe_3O_4/Ag NH

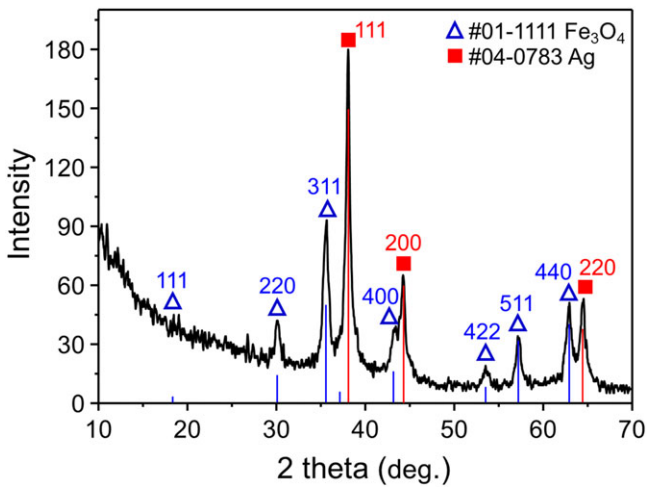

FIGURE 3 XRD pattern of rGO/Fe_3O_4/Ag NH

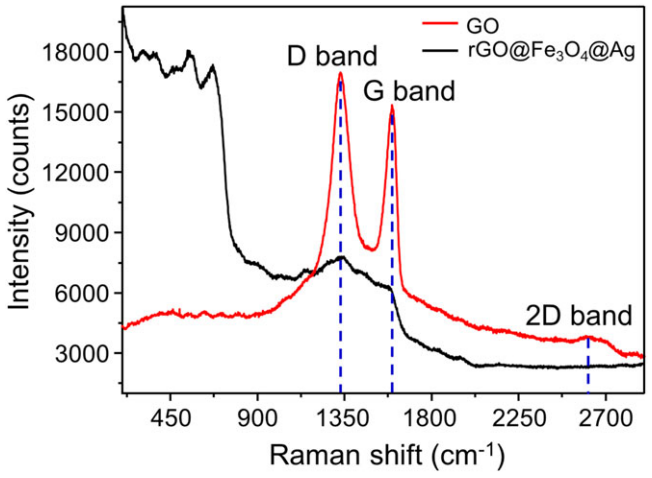

FIGURE 4 Raman spectra of GO and rGO/Fe_3O_4/Ag NH

which is weaker and broader than the D band. The Raman spectrum of rGO/Fe_3O_4/Ag NH also displays D band and G band at similar wavenumbers but their intensities are much weaker and not as well resolved as those of GO. This observation is acceptable because rGO only accounts for *ca* 15.38 wt% of rGO/Fe_3O_4/Ag NH (mass ratio of rGO:Fe_3O_4:Ag is 1.0:4.0:1.5). rGO is decorated and covered by Fe_3O_4 and Ag NPs, making the surface less accessible to laser excitation. In addition, the Raman spectrum of rGO/Fe_3O_4/Ag NH exhibits multiple and overlapped bands, which could be assigned to the symmetries of A_{1g} (670 cm^{-1}), E_g (308 cm^{-1}) and T_{2g} (542, 460 and 365 cm^{-1}) vibrational modes of Fe_3O_4.[34] These observations indicate that rGO/Fe_3O_4/Ag NH had been successfully synthesized.

3.5 | TEM analysis

Morphology and distribution of Fe_3O_4 and Ag NPs on the surface of rGO were studied using TEM. Figure 5(a) and (b) clearly illustrate that Fe_3O_4 and Ag NPs are well grown on the lateral surface of rGO sheets, indicating that our method is efficient for the synthesis rGO/Fe_3O_4/Ag ternary NH. Fe_3O_4 NPs uniformly cover the entire surface of rGO sheets with a high density and narrow size distribution (8–16 nm). The size of Ag NPs falls into the range 18–40 nm, which is typical for citrate-based synthesis of silver.[28] The (111) lattice planes of crystalline silver can be clearly observed in Figure S1. In comparison with grain

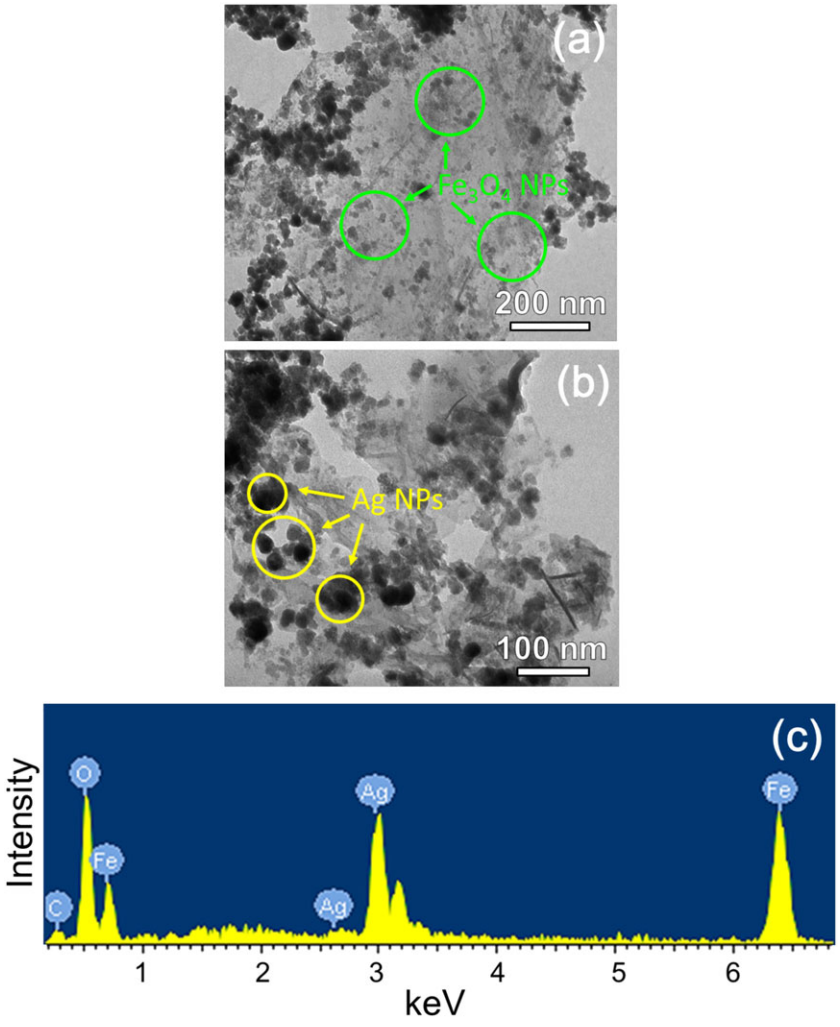

FIGURE 5 (a, b) TEM images and (c) SEM–EDX spectrum of rGO/Fe_3O_4/Ag NH

sizes calculated using Scherrer's formula mentioned in Section 2.3 (12.8 nm for Fe_3O_4 and 17 nm for Ag), these results suggest that rGO/Fe_3O_4/Ag NH consists of monocrystalline Fe_3O_4 NPs and polycrystalline Ag NPs.

3.6 | SEM–EDX analysis

The elemental composition of rGO/Fe_3O_4/Ag NH was quantitatively analyzed at the microscale using SEM–EDX. All elements (C, O, Fe and Ag) are detected, as shown in the EDX spectrum of rGO/Fe_3O_4/Ag NH in Figure 5(c). Table 1 presents the results of analysis at six different positions in the sample. The average weight percentages of each element are 2.25% (C), 28.47% (O), 45.27% (Fe) and 24.01% (Ag). Assuming the sample contains pure phases of rGO, Fe_3O_4 and Ag, their calculated mass percentages are 13.47% (rGO), 62.52% (Fe_3O_4) and 24.01% (Ag). As described in Section 1, the GO:Fe_3O_4:Ag mass ratio is approximately 1.0:4.0:1.5 based on the feed ratio, which is theoretically equal to 15.38%:61.54%:23.60%. We note that the mass percentage of rGO in the obtained rGO/Fe_3O_4/Ag NH must be smaller than that of GO, because the reduction of GO to rGO results in a decrease of oxygen mass percentage. Taking this into account, it can be concluded that the result of SEM–EDX elemental analysis is very close to that of theoretical calculation. This fact shows that the preparation of rGO/Fe_3O_4/Ag NH adopting our green method is very efficient in terms of composition control.

3.7 | Magnetic properties

The magnetization curve shown in Figure 6 indicates that rGO/Fe_3O_4/Ag NH exhibits superparamagnetic-like behavior at room temperature. The saturation magnetization (M_s) of rGO/Fe_3O_4/Ag NH is *ca* 29 emu g^{-1} at 12 kOe which is slightly smaller than that of rGO/Fe_3O_4 NH (39.2 emu g^{-1} at a mass ratio of 3.83),[27] obviously because of lower magnetite content. We have previously shown that for practical applications, the M_s value of rGO/Fe_3O_4 NH can be conveniently tuned by controlling rGO:Fe_3O_4 mass ratio. The superparamagnetic behavior provides evidence that the

TABLE 1 Elemental composition of rGO/Fe_3O_4/Ag NH from SEM–EDX analysis

Element	Amount at different positions (wt%)						Average (wt%)
	1	2	3	4	5	6	
C K	3.14	2.41	2.57	2.22	1.8	1.38	2.25
O K	33.34	32.12	26.88	28.37	23.5	26.63	28.47
Fe K	42.93	45.07	44.95	41.06	50.01	47.61	45.27
Ag L	20.58	20.4	25.61	28.35	24.69	24.39	24.01
All							100.00

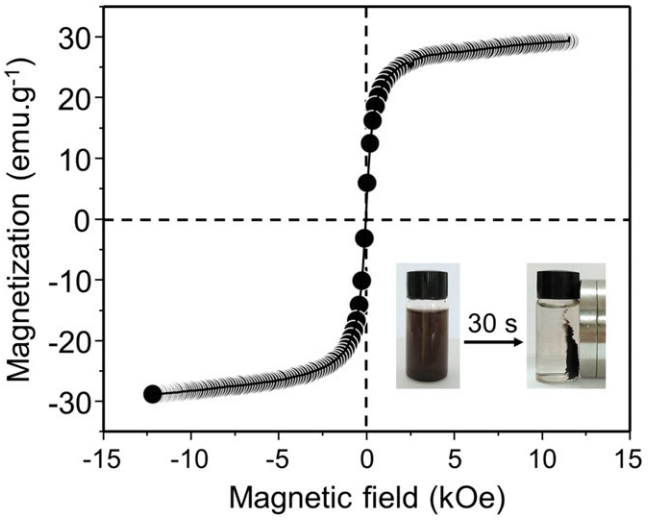

FIGURE 6 Magnetization curve of rGO/Fe_3O_4/Ag NH. Inset photos: aqueous suspension of rGO/Fe_3O_4/Ag NH before (left) and after (right) placing near a magnet for 30 s

Fe_3O_4 NPs deposited over rGO maintain their crystalline structure, and subsequent Ag deposition does not alter the magnetic properties of crystalline magnetite NPs. As a result, rGO/Fe_3O_4/Ag NH is readily manipulated using an external magnetic field. As shown in the inset of Figure 6, rGO/Fe_3O_4/Ag NH is easily separated from aqueous suspension upon exposure to a permanent magnet with a magnetic field of 0.5 T. This property makes rGO/Fe_3O_4/Ag NH promising for many applications in catalytic, biological and environmental fields. In this work, we investigated its application as a recoverable catalyst for the reduction of 4-NP.

3.8 | Catalytic study

The coupling of silver and magnetic graphene makes rGO/Fe_3O_4/Ag NH a potential magnetically recoverable catalyst. The catalytic activity of rGO/Fe_3O_4/Ag NH was studied using the transformation of 4-NP to 4-AP as a model reaction with $NaBH_4$ utilized as a reducing agent. The chosen reaction is also practically important because the US Environmental Protection Agency lists 4-NP as 'Priority Pollutant', while 4-AP is the final intermediate in the industrial synthesis of paracetamol.[35] In this reaction, 4-NP reacts with $NaBH_4$ to form pale yellow 4-nitrophenolate (4-NPL). Then, 4-NPL is reduced by excess $NaBH_4$ to form bright yellow 4-aminophenolate (4-APL) which is the basic form of 4-AP (in $NaBH_4$ solution). Therefore, the reduction of 4-NPL can be conveniently monitored with UV–visible absorption spectroscopy. Previous studies have shown that in the absence of catalyst, the color of 4-NPL solution remains unaltered for hours.[6]

Figure 7(a) shows digital photos of aqueous solutions containing 4-NP and $NaBH_4$ (without and with

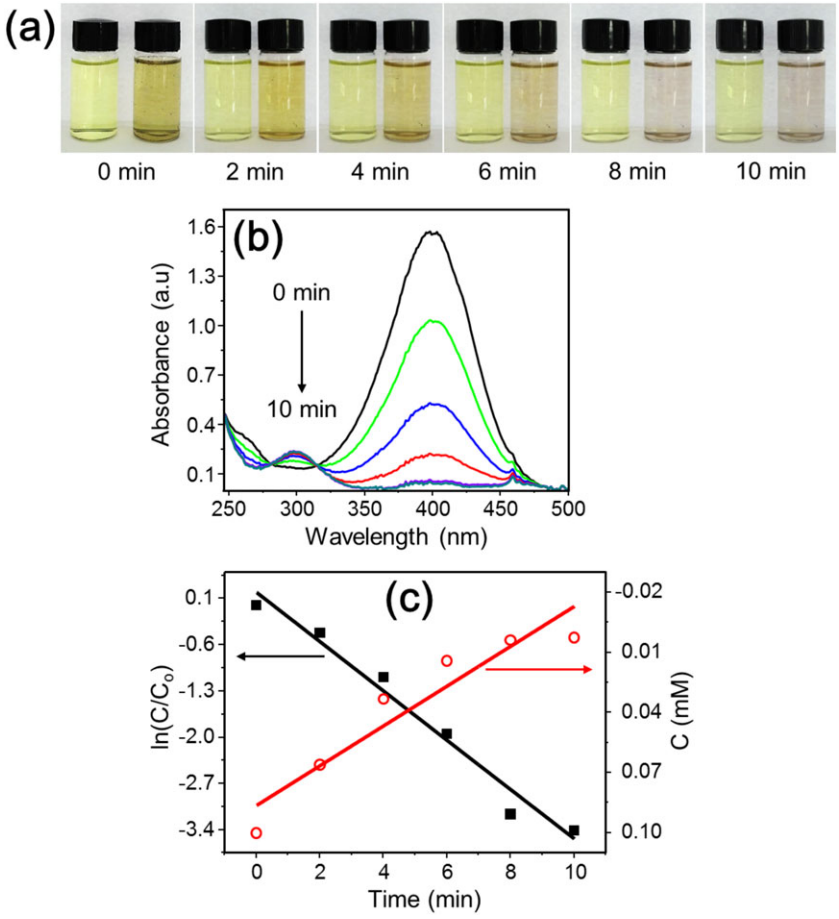

FIGURE 7 (a) digital photos of aqueous solutions of 4-NP reduced using $NaBH_4$ taken at various durations. In each photo, the left-hand bottle is without catalyst and the right-hand one is with rGO/Fe_3O_4/Ag NH catalyst. (b) time-dependent UV–visible spectra of aqueous solution of 4-NP catalytically reduced using $NaBH_4$. (c) linear fitting of concentration C and $\ln(C/C_0)$ versus reaction time

rGO/Fe_3O_4/Ag NH) taken at 0, 2, 4, 6, 8 and 10 min after mixing. The concentrations of 4-NP, $NaBH_4$ and rGO/Fe_3O_4/Ag NH are described in Section 1. After 10 min, the solution without catalyst retains its yellow color, while the solution with rGO/Fe_3O_4/Ag NH becomes transparent, indicating the high-yield conversion of 4-NPL to 4-APL.

Figure 7(b) shows time-dependent UV–visible spectra of solution containing 4-NP, $NaBH_4$ and rGO/Fe_3O_4/Ag NH. The reaction progress can be observed through the reduction in the intensity of adsorption band of 4-NPL at 400 nm. Simultaneously, the formation of 4-APL is evidenced by the occurrence of an increasing peak at *ca* 300 nm. The kinetics of the catalyzed reaction was evaluated by plotting and linearly fitting UV–visible absorption data by means of the least-squares method. Figure 7(c) shows plots of $\ln(C/C_0)$ and C versus reaction time for the reduction of 4-NPL over rGO/Fe_3O_4/Ag NH. The fitting of $\ln(C/C_0)$ versus reaction time shows better adjusted R^2 value (0.97) as compared with that of C versus reaction time (0.87), indicating that the catalytic reaction is appropriately described using pseudo-first-order kinetics. This is acceptable because the concentration of $NaBH_4$ (8 mM) is 80 times higher than that of 4-NP (0.1 mM); the surface of the solid catalyst (rGO/Fe_3O_4/Ag NH) is considered to be constant during the reaction; therefore the rate of the reaction depends on the concentration of only one reactant (4-NP). The derived apparent rate constant is $k = 0.373\ \text{min}^{-1}$ with a standard deviation of $0.031\ \text{min}^{-1}$. The half-life of 4-NP in the presence of rGO/Fe_3O_4/Ag NH is calculated to be 1.86 min, according to the formula

$$t_{1/2} = \frac{\ln 2}{k}$$

Table 2 presents a comparison of rate constants of the reduction of nitrophenols using several silver-based catalysts reported previously. Compared with other silver

TABLE 2 Comparison of rate constants for various silver-based catalysts

Catalyst	Apparent rate constant (min^{-1})	Ref.
Ag dendrites	0.34	[36]
rGO/Ag	0.49	[37]
Fe_3O_4/Ag	0.24	[38]
PG/Ag	0.33	[39]
PSMAA/Ag	0.19–0.49	[40]
rGO/Fe_3O_4/Ag	0.85–1.60	[19]
rGO/Fe_3O_4/Ag	0.25–0.69	[18]
rGO/Fe_3O_4/Ag	0.37	This study

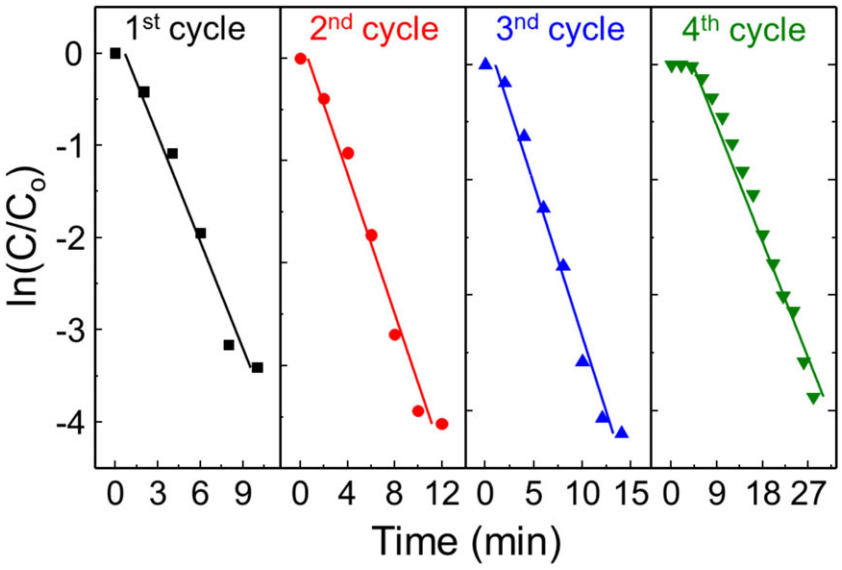

FIGURE 8 Catalytic reduction of 4-NP for four consecutive cycles over rGO/Fe_3O_4/Ag NH

nanoparticle-based catalysts, the rGO/Fe_3O_4/Ag NH has comparable performance, while it can be recovered.

The separability and reusability of the hybrid catalyst were also examined. After each reaction, rGO/Fe_3O_4/Ag NH was magnetically separated, thoroughly washed and introduced to a new solution of 4-NP for the next catalytic experiment. Figure 8 shows plots of $\ln(C/C_0)$ versus reaction time for four consecutive cycles. All plots can be linearly fitted, indicating that the catalytic reaction is appropriately described using pseudo-first-order kinetics. The conversion efficiency is calculated according to the formula

$$\eta = \frac{C_0 - C}{C_0} \times 100\%$$

It is calculated that the conversion efficiency upon completion of our experiments is 96.7% (first cycle, at 10 min), 97.2% (second cycle, at 12 min), 95.5% (third cycle, at 14 min) and 94.4% (fourth cycle, at 28 min). These data suggest that the catalytic activity of rGO/Fe_3O_4/Ag NH is retained well for the first three cycles then decreases from the fourth cycle, possibly due to the loss of active catalyst during separation and washing processes. In addition, the occurrence of an induction period is also observed at the fourth cycle (*ca* 4 min), which practically means that it would take a longer time for the catalyst to be active. A TEM image of rGO/Fe_3O_4/Ag NH after the fourth cycle (Fig. S2) shows that the morphology is almost unchanged. Therefore, the induction period is thought to be connected to changes in surface composition and oxidation state of the catalyst, which should be the subject of further rigorous experiments.

4 | CONCLUSIONS

In summary, we successfully prepared rGO/Fe_3O_4/Ag NH through a novel, simple, inexpensive and green route, using sodium citrate as a reducing agent. Fe_3O_4 and Ag NPs were well grown on rGO sheets at high densities. Consequently, rGO/Fe_3O_4/Ag NH simultaneously exhibited good magnetic property (saturated magnetization of 29 emu g^{-1} at 12 kOe) and high catalytic activity towards the reduction of 4-NP (rate constant of 0.37 min^{-1}) even after multiple uses. As a result, rGO/Fe_3O_4/Ag NH could potentially be used as a magnetically recoverable catalyst in the reduction of 4-NP and for environmental remediation.

ACKNOWLEDGMENTS

This research was funded by the Vietnam National Foundation for Science and Technology Development (NAFOSTED) under grant number 103.02-2015.100. Financial support from Le Quy Don University, grant no. 14.0. A.04, is gratefully acknowledged. We thank AMT Co. Ltd (Hanoi, Vietnam) for providing graphite flakes.

REFERENCES

[1] D. Wang, D. Astruc, *Chem. Rev.* **2014**, *114*, 6949.

[2] B. Karimi, F. Mansouri, H. M. Mirzaei, *ChemCatChem* **2015**, *7*, 1736.

[3] R. Dalpozzo, *Green Chem.* **2015**, *17*, 3671.

[4] M. Nasrollahzadeh, S. Mohammad Sajadi, A. Rostami-Vartooni, M. Khalaj, *J. Mol. Catal. A* **2015**, *396*, 31.

[5] P. V. Kamat, *J. Phys. Chem. Lett.* **2009**, *1*, 520.

[6] T. V. Thu, P. J. Ko, N. H. H. Phuc, A. Sandhu, *J. Nanopart. Res.* **2013**, *15*, 1.

[7] T. Thu, A. Sandhu, *AIP Conf. Ser.* **2014**, *1585*, 136.

[8] Y. Zhang, S. Liu, W. Lu, L. Wang, J. Tian, X. Sun, *Catal. Sci. Technol.* **2011**, *1*, 1142.

[9] W. Lu, R. Ning, X. Qin, Y. Zhang, G. Chang, S. Liu, Y. Luo, X. Sun, *J. Hazard. Mater.* **2011**, *197*, 320.

[10] G. Williams, B. Seger, P. V. Kamat, *ACS Nano* **2008**, *2*, 1487.

[11] S. Bong, Y.-R. Kim, I. Kim, S. Woo, S. Uhm, J. Lee, H. Kim, *Electrochem. Commun.* **2010**, *12*, 129.

[12] W. Lu, Y. Luo, G. Chang, X. Sun, *Biosens. Bioelectron.* **2011**, *26*, 4791.

[13] S. Wu, Q. He, C. Zhou, X. Qi, X. Huang, Z. Yin, Y. Yang, H. Zhang, *Nanoscale* **2012**, *4*, 2478.

[14] J. Hu, Y. Wang, M. Han, Y. Zhou, X. Jiang, P. Sun, *Catal. Sci. Technol.* **2012**, *2*, 2332.

[15] F. Chen, Y. Wang, Q. Chen, L. Han, Z. Chen, S. Fang, *Mater. Res. Express* **2014**, *1*, 045049.

[16] J. Hu, Y.-l. Dong, X.-j. Chen, H.-j. Zhang, J.-m. Zheng, Q. Wang, X.-g. Chen, *Chem. Eng. J.* **2014**, *236*, 1.

[17] K. Liang, X. Li, S.-Z. Kang, L. Qin, G. Li, J. Mu, *Carbon* **2014**, *80*, 716.

[18] Z. Ji, X. Shen, X. Yue, H. Zhou, J. Yang, Y. Wang, L. Ma, K. Chen, *J. Colloid Interface Sci.* **2015**, *459*, 79.

[19] J.-c. Qu, C.-l. Ren, Y.-l. Dong, Y.-p. Chang, M. Zhou, X.-g. Chen, *Chem. Eng. J.* **2012**, *211–212*, 412.

[20] W. Lu, F. Liao, Y. Luo, G. Chang, X. Sun, *Electrochim. Acta* **2011**, *56*, 2295.

[21] X. Sun, S. Dong, E. Wang, *Macromolecules* **2004**, *37*, 7105.

[22] G. Chang, Y. Luo, W. Lu, X. Qin, A. M. Asiri, A. O. Al-Youbi, X. Sun, *Catal. Sci. Technol.* **2012**, *2*, 800.

[23] M. Zong, Y. Huang, H. Wu, Y. Zhao, S. Wang, N. Zhang, W. Zhang, *Mater. Lett.* **2013**, *111*, 188.

[24] G. Liu, W. Jiang, Y. Wang, S. Zhong, D. Sun, J. Liu, F. Li, *Ceram. Int.* **2015**, *41*, 4982.

[25] H.-Z. Zhang, C. Zhang, G.-M. Zeng, J.-L. Gong, X.-M. Ou, S.-Y. Huan, *J. Colloid Interface Sci.* **2016**, *471*, 94.

[26] N. Wang, B. Hu, M.-L. Chen, J.-H. Wang, *Nanotechnology* **2015**, *26*, 195703.

[27] T. V. Thu, A. Sandhu, *Mater. Sci. Eng., B* **2014**, *189*, 13.

[28] Z. Zhang, H. Chen, C. Xing, M. Guo, F. Xu, X. Wang, H. J. Gruber, B. Zhang, J. Tang, *Nano Res.* **2011**, *4*, 599.

[29] Y. Si, E. T. Samulski, *Nano Lett.* **2008**, *8*, 1679.

[30] S. Stankovich, R. D. Piner, S. T. Nguyen, R. S. Ruoff, *Carbon* **2006**, *44*, 3342.

[31] Y. Xu, H. Bai, G. Lu, C. Li, G. Shi, *J. Am. Chem. Soc.* **2008**, *130*, 5856.

[32] R. Waldron, *Phys. Rev.* **1955**, *99*, 1727.

[33] K. N. Kudin, B. Ozbas, H. C. Schniepp, R. K. Prud'homme, I. A. Aksay, R. Car, *Nano Lett.* **2008**, *8*, 36.

[34] O. N. Shebanova, P. Lazor, *J. Solid State Chem.* **2003**, *174*, 424.

[35] F. Ellis, *Paracetamol: A Curriculum Resource*, Royal Society of Chemistry, Cambridge **2002**.

[36] W. Zhang, F. Tan, W. Wang, X. Qiu, X. Qiao, J. Chen, *J. Hazard. Mater.* **2012**, *217–218*, 36.

[37] Y. Li, Y. Cao, J. Xie, D. Jia, H. Qin, Z. Liang, *Catal. Commun.* **2015**, *58*, 21.

[38] K. S. Shin, Y. K. Cho, J.-Y. Choi, K. Kim, *Appl. Catal. A* **2012**, *413–414*, 170.

[39] B. Baruah, G. J. Gabriel, M. J. Akbashev, M. E. Booher, *Langmuir* **2013**, *29*, 4225.

[40] G. Liao, J. Chen, W. Zeng, C. Yu, C. Yi, Z. Xu, *J. Phys. Chem. C* **2016**, *120*, 25935.

SUPPORTING INFORMATION

Additional Supporting Information may be found online in the supporting information tab for this article.

How to cite this article: Thu TV, Ko PJ, Nguyen TV, Vinh NT, Khai DM, Lu LT. Green synthesis of reduced graphene oxide/Fe_3O_4/Ag ternary nanohybrid and its application as magnetically recoverable catalyst in the reduction of 4-nitrophenol. *Appl Organometal Chem*. 2017;e3781. https://doi.org/10.1002/aoc.3781